Anthropol. Anz. 75/2 (2018), 113–130
J. Biol. Clin. Anthropol.
Published online 31 January 2018, published in print May 2018

Article

Complex pattern of variation in neurocranial ontogeny revealed by CT-scanning

Marisol Anzelmo[1,*], Fernando Ventrice[2], Diana Kelmansky[3], and Marina Sardi[1]

[1] División Antropología, CONICET, Museo de La Plata. Facultad de Ciencias Naturales y Museo. Universidad Nacional de La Plata. La Plata, Buenos Aires, Argentina. 1900
[2] Hospital Posadas. Buenos Aires, Argentina
[3] Instituto de Cálculo. Facultad de Ciencias Naturales y Exactas. Universidad de Buenos Aires. Buenos Aires, Argentina
* Corresponding author: manzelmo@fcnym.unlp.edu.ar

With 7 figures and 7 tables

Abstract: The neurocranium of hominid species has been largely studied with reference to the midsagittal plane, with variations being attributed to brain evolution. By contrast, there is limited information on variation in non-midsagittal regions, which are the points of insertion of muscles and bony structures related to mastication. This work aims to analyze ontogenetic changes and sexual dimorphism (SD) in midsagittal and non-midsagittal neurocranial structures from a contemporary human sample comprising 138 computed tomography (CT) cranial images of individuals ranging from infants to adults. Morphology of the vault and the base was assessed by registering landmarks and semilandmarks, which were analyzed by geometric morphometrics, and the endocranial volume (EV). The results of regressions and Kruskal-Wallis test indicate that the major size and shape changes in both midsagittal and non-midsagittal regions occur during infancy and juvenility; shape changes are also associated with an increase in EV. The size of the midsagittal vault, the shape of the non-midsagittal vault and the size of the base show an extension of ontogenetic trajectories. Sexes show similar changes in shape but different changes in size. We conclude that brain growth appears to be an important factor influencing the morphology of the neurocranium, at least during infancy and childhood. Subsequent changes may be attributed to osteogenic activity and the differential growth of the brain lobes. Masticatory-related bony structures and muscles may not be strong enough factors to induce independent modifications in non-midsagittal structures. The small influence of the cranial muscles would explain why the human neurocranium is a quite integrated structure.

Keywords: growth and development; modern human; modularity; functional matrices

Introduction

The neurocranium is a variable structure among primates. Within the hominid lineage the most important neurocranial changes involve a more globular morphology. This has been attributed to the development of a large brain and a reduction in the masticatory muscles, which in turn is linked to less developed superstructures (Lieberman et al. 2004). Classic anthropological studies have compared human populations using the cephalic index (CI), calculated by dividing the maximum head breadth by length and multiplying by 100 (CI = (width/breadth)*100). The linear distance between cranial points were measured to estimate head breadth (i.e. eurion-eurion distance) and head length (i.e. glabella-opisthocranion distance) (Howells 1973). Based on this typological approach, populations were classified over a wide range, from dolicocephalic (long-headed) to brachycephalic (short-headed) for taxonomic purposes (Imbelloni 1938). Most of these studies were carried out on adults and did not provide any insight into the biological mechanisms underlying a given morphology.

Over recent decades, the ontogenetic variation in the morphology of the neurocranium has been investigated to elucidate how morphological differences arise among adults and how ontogeny contributes to variations between and within populations and between related species (Richtsmeier et al. 1993; Ackermann & Krovitz 2002; Strand-Vidarsdóttir et al. 2002; Buschang & Hinton 2005). Research dealing with neurocranium changes during ontogeny in modern humans has largely focused on the analysis of midsagittal structures (Bookstein et al. 1999; Bookstein et al. 2003; Bruner et al. 2004). The midsagittal region is usually delimited by a plane defined by three midline points (Bookstein et al. 1999; Bookstein et al. 2003; Bruner et al. 2004; Balzeau 2006).

DOI: 10.1127/anthranz/2018/0771
www.schweizerbart.de
0003-5548/2018/0771 $ 4.50

The results from these studies suggest that the most important changes in size and shape are detected during the first 2 years of postnatal life, with minor changes up to about 6 years of age (Lieberman et al. 2000; Lieberman et al. 2002; Bastir et al. 2005; Bastir et al. 2006; Anzelmo et al. 2013). Such changes have been attributed to brain growth (Bastir et al. 2006), exhibiting a sharp increase over the first 3 years of postnatal life and attaining most of its adult size before 6 years of age (Guihard-Costa & Ramirez-Rozzi 2004; Lenroot & Giedd 2006; Giedd et al. 2009; Ventrice 2011). In contrast to ontogenetic changes in the growth of neurocranial midsagittal structures, those involving non-midsagittal structures are poorly known. In this study non-midsagittal regions include neurocranium structures lateral to the midsagittal plane.

Few studies (Bastir et al. 2005; Bastir et al. 2006; Bastir & Rosas 2009; Anzelmo et al. 2014) have proposed that non-midsagittal structures show a different ontogeny, suggesting that the neurocranium is organized into development modules. A module is considered a unit, whose parts have stronger interactions among them than with parts belonging to other modules (Klingenberg 2009). For instance, the glenoid cavity of the basicranium develops until adolescence, taking longer period to grow compared to midsagittal basicranial structures. This result was interpreted by Bastir et al. (2005; 2006) and Bastir & Rosas (2006; 2009) as evidence of integration between the mandibular ramus and the glenoid cavity, both of which are involved in mastication (Bastir & Rosas 2005; Bastir et al. 2006). Therefore, non-midsagittal basicranial structures seem to be more integrated with the jaw than midsagittal ones, following a pattern of facial development because they undergo changes in size and shape up to adolescence (Bastir et al. 2006). However, a limitation of these conclusions is that changes were analyzed from lateral radiographs (Bastir et al. 2005; Bastir et al. 2006).

On the other hand, little is known about the non-midsagittal developmental traits of the vault. The walls of the cranial vault, which serve as attachment for the temporal muscles, show a low proportion of adult size at birth and grow over a long period of time; they experience an increase in growth rate after the eruption of the first deciduous molars because of their importance in chewing (Sperber 2010). In analyzing the ectocranial surface of the human vault, Anzelmo et al. (2013) observed that midsagittal and lateral traits express coordinated shape modifications and attain adult shape at early adolescence. Such a high integration was interpreted as the result of the influence of a single factor -brain growth- on the vault (Anzelmo et al. 2013; Barbeito-Andrés et al. 2015).

Sexual dimorphism (SD) in neurocranium morphology has also been poorly studied. Most studies on SD have mainly dealt with facial skeleton. In this context, it is well known that differences in the facial skeleton between adult males and females are explained by divergence in cranial ontogeny (Baughan & Demirjian 1978; Humphrey 1998; Bulygina et al. 2006; González et al. 2009; Strand-Vidarsdóttir & O'Higgins 2001), differences present at birth and a longer growth period in males than in females. It is also accepted that the neurocranium is a sexually dimorphic region (Ricklan & Tobias 1986; Rushton 1992; Buikstra & Ubelaker 1994), with that of males being larger and having more developed superstructures.

Research on human neurocranium has traditionally relied on physical measurements using dried skulls or radiographs. In recent decades, 3D technologies have been applied to the fields of biological and forensic anthropology. In particular, computed tomography (CT) scanning became a useful tool for morphological analysis. Indeed, 3D reconstructions of the endocranial surface of both non-human primates (Neubauer et al. 2010; Sardi et al. 2014; Zollikofer et al. 2016) and humans (Neubauer et al. 2009; Zollikofer et al. 2016) allowed assessing changes in size and shape from newborn to adults. However, previous studies of neurocranial morphology have focused on midsagittal variation, excluding non-midsagittal structures from the analysis (Bastir et al. 2005; Bastir et al. 2006; Bastir & Rosas 2009; Anzelmo et al. 2013). In this study we aim to examine the ontogeny and SD of the neurocranium in a modern human sample from a midsagittal and non-midsagittal perspective and to determine their relationship during ontogenesis.

We tested the following hypotheses: (1) Hypothesis 1 (H1), the midsagittal and non-midsagittal neurocranial regions follow different ontogenetic trajectories, and based on previous studies, it is expected that a) non-midsagittal structures attain adult size and shape later than midsagittal ones; b) shape variation is more associated with endocranial volume (as a proxy for brain size) in the midsagittal than in the non-midsagittal region; and c) differentiation between these regions is more pronounced at the base than in the vault. (2) Hypothesis 2 (H2), the ontogenetic trajectories of the neurocranium are significantly different between males and females, and it is expected that d) an important proportion of SD occurs during postnatal ontogeny.

Material and methods

Sample

We used a sample of 138 CT cranial images of modern humans of both sexes from 0 to 32 years old. The dataset was constructed at FLENI (Fundación para la Lucha contra las Enfermedades Neurológicas de la Infancia, Buenos Aires, Argentina) by Dr. Fernando Ventrice, who used it in his PhD (Ventrice 2011). FLENI is a non-profit organization dedicated to the prevention, diagnosis, treatment and research of neurological diseases affecting individuals of all ages, who come from different regions of Argentina, mostly urban areas. The sample was composed of patients who approached FLENI showing possible neurorogical clinical symptoms. In this context, the doctors advised the patients

to undergo a CT scan. Only patients with no neurological involvement (N = 138) were included in the database, which was constructed over one year. To use the CT images for research purposes, they were anonymized in accordance with the requirements of the ethics committee of the institution. This process involves stripping patient identifiers such as name, date of birth, address, etc.

Taking into account several traits of body and behavioral maturation such as brain growth, tooth eruption, sexual and cognitive development, etc, the sample was divided into four age groups (Bogin 1999; Bogin 2003): infant–child (0–5.99 years old), juvenile (6–11.99 years old), adolescent (12–17.99 years old), and adult (18–32 years old). Sample size and sex distribution are displayed in Table 1. Unlike Bogin (1999), who distinguished between infants (0–2 years old) and children (3–6 years old), we pooled them together since they would have been underrepresented among groups, thereby hindering statistical analysis.

Table 1. Sample size by ontogenetic stage and sex.

Age groups (years old)	Males	Females	Total
Infant-child (0–5.99)	12	7	19
Juvenile (6–11.99)	14	11	25
Adolescent (12–17.99)	12	15	27
Adult (≥ 18)	20	47	67
Total	58	80	138

Data collection

Individuals were scanned using a General Electric Light Speed RT16; 275 axial CT images with a resolution of 512 × 512 pixels and a voxel size equal to 0.449 × 0. 449 × 0.625 mm were produced for each individual. All scans contained images of the neurocranium and superior facial skeleton. A three-dimensional (3D) superficial reconstruction was created from CT slices by choosing a density threshold that corresponds to the Hounsfield unit scale (Spoor et al. 2000). Surface extraction thresholds, which need to be defined to yield a reconstruction, were determined empirically. A threshold of 1,150 Hounsfield units was used to show the maximum amount of bony tissue with the least amount of distortion. CT images were analyzed with a trial version of AVIZO 6.0 (Visualization Science Group) for 3D data analysis, and morphometric software package TPS for 2D analysis.

To analyze midsagittal region morphology, a 2D cut plane defined by Nasion, Foramen caecum and Basion was extracted. We selected a 2D midsagittal plane for evolutionary and ontogenetic comparisons because it has been used in numerous studies. Besides, no additional biological information is provided by adding a third dimension (z-axis) because the midsagittal plane divides structures into two symmetrical parts.

In none of the original CT cuts the three points selected could be exactly traversed. Then, to obtain homologous images, we defined an algorithm that automatically rotates the original CT slices from each individual so that at least one of them is aligned with these points. The extracted 2D CT slices were imported and analyzed using the TPS morphometric software package.

The extracted 2D cuts were imported and analyzed with the TPS morphometric program package. Firstly, landmarks were 2D-digitized (Table 2; Fig. 1). Landmarks are defined as discrete anatomical loci that can be recognized as the same loci in all the individuals of the sample (Zelditch et al. 2004). Previously, we evaluated the intraobserver measurement error (ME) in locating each landmark. The measurement error is the difference between the recorded and true value of a variable (Arnqvist & Martensson 1998). To quantify and reduce ME, we randomly selected 14 individuals of different ages. The landmarks were digitized on two occasions two weeks apart. We decided not to evaluate the ME for semilandmarks because these were adjusted to minimize the bending energy by a sliding procedure after digitization, and as a result they were relocated from their original positions (see below). The landmark configurations of the different individuals were superimposed by carrying out a generalized Procrustes analysis separately for each measurement series, thus obtaining Procrustes-fit coordinates for the x- and y-axes of each landmark. A paired-samples t-test was performed to quantify the ME, using the coordinate of each axis as independent variable and each measurement series as grouping variable. This test was used because data of the different samples are not independent as they are derived from the same individual.

Secondly, evenly-spaced semilandmarks were placed onto the curve extended from Glabella to Bregma, Bregma to Lambda and Lambda to Opistion (Table 2; Fig. 1). Semilandmarks are frequently used to describe structures such as curves or surfaces, where landmarks are rare. They provide information on a single dimension – the one which is orthogonal to the curve – and are not homologous between individuals. Different superposition methodologies have been developed to reduce the influence that the distance between adjacent landmarks has on shape variation between individuals. In addition, these methods allow semilandmarks to be treated as landmarks in subsequent statistical analyses. There are two main superposition methodologies leading to (1) minimize bending energy, (2) minimize Procrustes distance. The present study involves an ontogenetic series, implying that we have to deal with a large morphological variation. Hence, the difference between results from methods (1) and (2) is very small compared to within-sample variability. We chose methodology (1) because, as opposed to (2), it retains some of the tangent variation to the curve (Gunz et al. 2005).

Table 2. Landmarks digitized on the neurocranium in the midsagittal region.

Nº	Name	Description	*Inn / Out	Vault / Base
1	Glabella	Most prominent point in the glabellar region where the skull is located according to Frankfurt plane	Out	Vault
7	Bregma	Midline point where midsagittal and coronal sutures intersect	Out	Vault
13	Lambda	Midline point where midsagittal and lamboidal sutures intersect	Out	Vault
23	Endobregma	Midline point where midsagittal and coronal sutures intersect on inner side	Inn	Vault
29	Endolambda	Midline point where midsagittal and lambdoidal sutures intersect on inner side	Inn	Vault
34	Inion	Point where midsagittal plane and superior nuchal lines intersect	Out	Base
37	Opisthion	Point where midsagittal plane and posterior edge of *foramen magnum* intersect	Out	Base
38	Basion	Point where midsagittal plane and anterior edge of *foramen magnum* intersect	Out	Base
39	Ecto-Sphenobasion	Point where midsagittal plane and sphenooccipital synchondrosis intersect	Out	Base
40	Hormion	Posterior border of vomer	Out	Base
41	Endinion	Point where midsagittal and transverse sinus intersect on inner side	Inn	Base
44	Endopisthion	Point where midsagittal plane and posterior edge of *foramen magnum* intersect on inner side	Inn	Base
45	Endobasion	Point where midsagittal plane and anterior edge of *foramen magnum* intersect on inner side	Inn	Base
46	Endo-sphenobasion	Point where midsagittal plane and sphenooccipital synchondrosis intersect on inner side	Inn	Base
47	Dorsum Sella	Most posterior point on internal contour of the sella turcica (or hypophyseal fossa)	Inn	Base
48	Sella	Center of sella turcica	Inn	Base
49	Pituitary point	Midsagittal point on *tuberculum sellae* located in front of sella turcica	Inn	Base
50	Sphenoidale	Most posterior, superior midline point of planum sphenoideum	Inn	Base
51	Planum sphenoideum point	Most superior midline point on sloping surface in which cribriform plate is set.	Inn	Base
52	Foramen Cecum	Pit on cribriform plate between *crista galli* and endocranial wall of frontal bone	Inn	Base

Reference numbers in Fig. 1; *Inn: inner surface; Out: outer surface

To analyze non-midsagittal neurocranial morphology, we tested a large number of 2D coronal slices but none of them allowed digitization of homologous points among individuals. The main problem to be solved was related to ontogenetic variation because the use of three landmarks to define the CT slice resulted in the representation of very distinct structures at different ages, which were not comparable especially in the basicanium. Therefore, we decided to digitize 3D internal and external landmarks and semilandmarks on the middle region of the neurocranium (Table 3; Fig. 2). This region was considered as the most optimal area for digitization of points because it allows to evaluate the influence of several factors (e.g. brain growth and mastication) on the morphological changes of the neurocranium (Susan Herring, personal communication). The mid-neurocranium includes the middle fossa of the base, temporal squama, and the anterior region of the parietal. To evaluate intraobserver ME in the digitized landmarks we followed the same procedure as with the midsagittal plane. In this case, the generalized Procrustes analysis also included the z-coordinate to analyze 3D point data. For the vault, a series of evenly-spaced semilandmarks were placed onto the curve extended from the Bregma to the Posterior Zygomatic point, which is the most posterior point on the zygomatic arc of the temporal bone (Fig. 2). Prior to the statistical analysis, semilandmarks were replaced along the outline curves using a linear interpolation between the original curve points (Reddy et al. 2004) to reduce the effect that the distance between landmarks has on the estimation of shape differences between individuals.

Geometric morphometric techniques were applied on the raw coordinate configurations of landmarks and semilandmarks in order to eliminate variation due to position, rotation and scale. In this context, shape was defined as the geometric information that remains once scale, position, and rotational

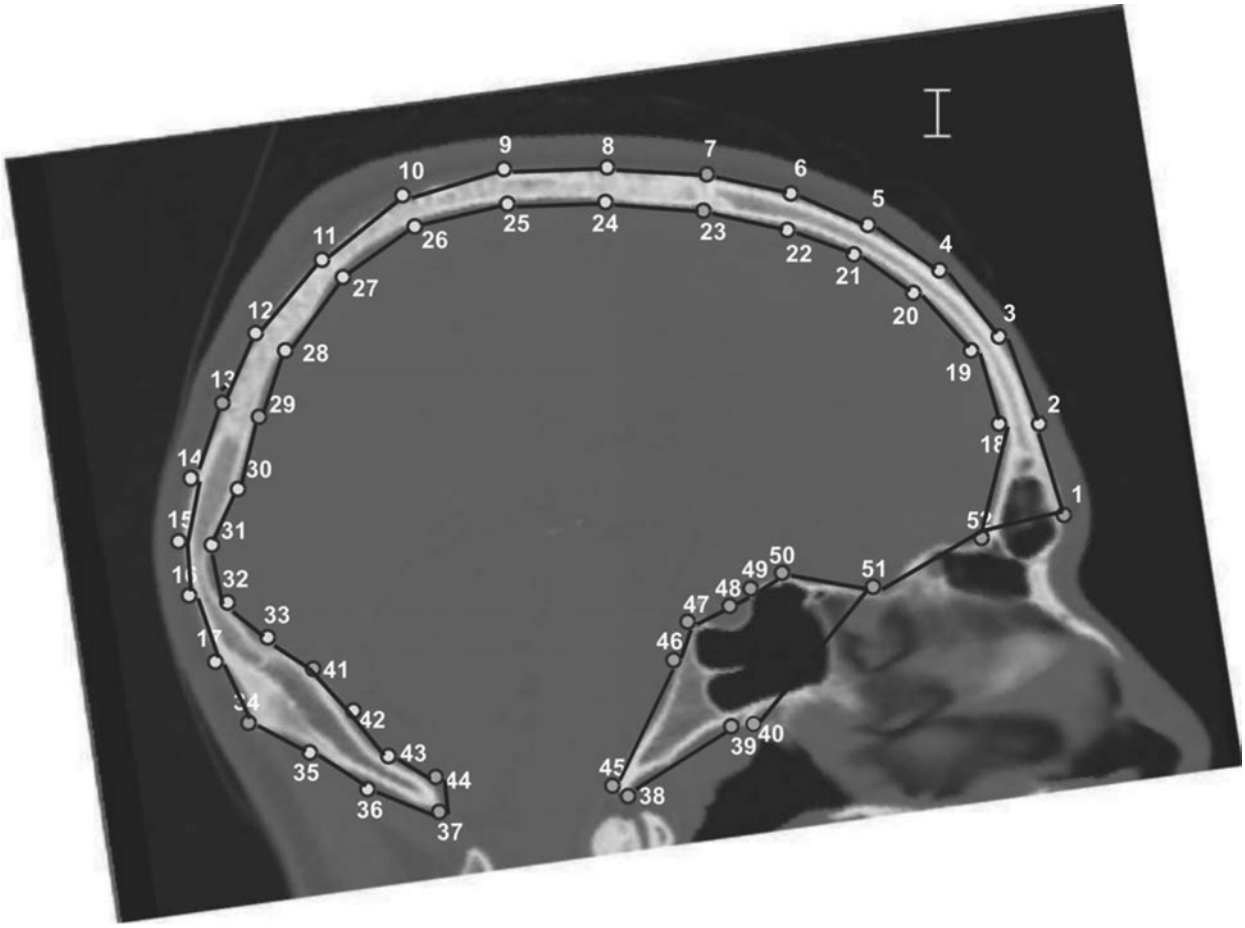

Fig. 1. Landmarks (dark gray) and semilandmarks (light grey) digitized on the midsagittal region. For full anatomical descriptions of each numbered landmark see Table 2. Wireframes (black) used to display shape change are shown.

effects were removed (Kendall 1977). Thus, form was studied from one size variable (Centroid Size, CS) and a set of shape variables (Procrustes coordinates).

For each cranium, the endocranial surface was digitally extracted from the CT images following the first method described by Bienvenu et al. (2011) and then a measure of endocranial volume (EV) was automatically calculated.

Data analysis

The midsagittal vault, midsagittal base, non-midsagittal vault and non-midsagittal base were independently analyzed using generalized Procrustes analysis. First, a Principal Components analysis (PCA) was carried out on the Procrustes coordinates. Following Mitteroecker et al. (2005) only PCs explaining more than 80% of variation were retained. Second, a correlation coefficient between each PC and the log-transformed age was obtained to identify axes of ontogenetic shape variation. We decided to retain for further analysis the PCs with a significant correlation with age and values of r equal to or greater than 0.5, as we consider that lower correlation values provide little information on ontogenetic shape variation. Third, we obtained trajectories by applying a piecewise linear regression analysis. In this method the independent X variable is divided into segments and the regression analysis is performed separately for these segments. The boundaries between the segments are called breakpoints (Vieth 1989). In this study, the CS and the selected PC scores were considered as dependent variables while age was considered as the independent variable, selecting three breakpoints at the limits of the ontogenetic groups (ages 6, 12 and 18 years). Slopes for each segment and statistically significant differences between contiguous slopes were assessed. Finally, the piecewise regression was repeated including sex as a group variable. In this case, the piecewise trajectory was obtained for males and females, but significant differences in the intercepts were assessed by fitting their CS values and PC scores to a common slope. If the group variable (i.e., sex) is significantly different, the piecewise trajectories of sexes are parallel, otherwise they overlap.

Since part of shape variation may be size-related (which is defined as allometry in the context of geometric

Table 3. Landmarks digitized on the neurocranium in the non-midsagittal region.

Nº	Name	Definition	*Inn/Out	Vault/Base
1	Bregma	Point where midsagittal plane and coronal suture intersect.	Out	Vault
10	Endobregma	Point where midsagittal plane and coronal suture intersect on inner side	Inn	Vault
19	External Petrosal Apex	Most medial point of petrosal portion of temporal on outer side	Out	Base
20	Carotic Canal	Most anterior point of carotic canal	Out	Base
21	Foramen Spinosum	Most anterior point of foramen spinosum	Out	Base
22	Foramen Ovale	Most anterior point of foramen ovale	Out	Base
23	Sphenotemporal	Most external point of groove located in front of sphenotemporal crest	Out	Base
24	Parietomastoid	Point where mastoid portion of temporal, temporal squama and parietal intersect	Out	Base
25	Ecto-sphenobasion	Point where midsagittal plane and sphenooccipital suture intersect on outer side	Out	Base
26	Posterior zygomatic point	Most posterior point of zygomatic arch on temporal	Out	Base
27	Internal Petrosal Apex	Most medial point of petrosal portion of temporal on inner side	Inn	Base
28	Internal Acoustic Porus	Point on superomedial border of acoustic porus	Inn	Base
29	Foramen Spinosum	Most anterior point of foramen spinosum	Inn	Base
30	Foramen Ovale	Most anterior point of foramen ovale	Inn	Base
31	Sphenoid Wing	Maximal 3D curvature of greater sphenoid wings	Inn	Base
32	Petrosal base	Point where posterior border of petrosal portion and temporal-occipital suture intersect	Inn	Base
33	Endo-sphenobasion	Point where midsagittal plane and sphenooccipital suture intersect on inner side	Inn	Base

Reference numbers in Fig. 2; *Inn: inner surface; Out: outer surface

morphometrics, Klingenberg 2016) we also evaluated the association between shape and EV. EV is recognized as an indicator of brain size, providing an estimation of overall size when soft tissues are not available (Conroy et al. 2000; Bienvenu et al. 2011). Firstly, a piecewise linear regression analysis was performed, with EV as the dependent variable and age as the independent variable. Secondly, a linear regression analysis was conducted between contiguous ontogenic groups -infancy-childhood/juvenility, juvenility/adolescence, adolescence/adulthood-, with PCs scores as the dependent variable and the EV as the independent variable.

Finally, a non-parametric Kruskal-Wallis test was used to analyze differences in CS values and PC scores among all age groups, followed by a post-hoc test. To determine the age of maturation more accurately, the juvenile and adolescent groups were subdivided into smaller age groups of adequate sample size, following Bastir et al. (2006) and Anzelmo et al. (2013).

Visualization of shape change

Shape variation from birth to adulthood was shown as changes in the relative positions of landmarks and semilandmarks through wireframe deformation. The consensus configuration was indicated in gray color. The youngest individuals on one side and the eldest individuals on the other, compared with the consensus configuration, were considered as targets (shown in black).

Results

Intraobserver error

Tables 4 and 5 show the results obtained from the paired t-test for the landmarks of the midsagittal and non-midsagittal regions, respectively. Significant differences between the series were only detected for two landmarks, one in the y-axis of the Endobregma (number 8) in the midsagittal region and the other in the x- and z-axes of the Posterior Zygomatic (number 26) in the non-midsagittal region. To solve this problem, the definition of these landmarks was improved and they were digitized again. This procedure continued until differences in ME were no longer statistically significant between the series.

Ontogenetic size variation

The midsagittal features of the vault and base followed similar growth trajectories, with sizes increasing from infancy to early adulthood. For the vault, piecewise regression analy-

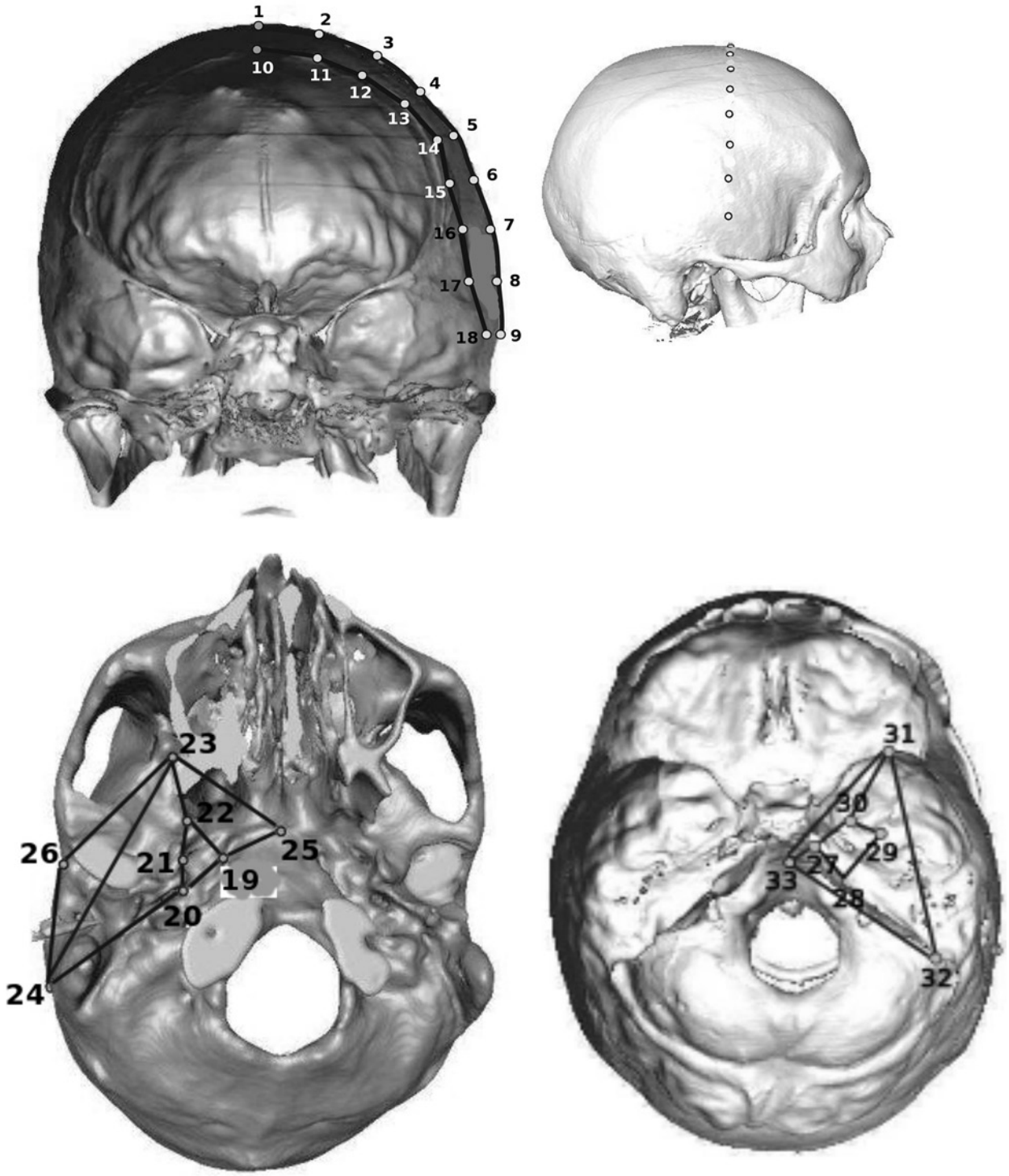

Fig. 2. Landmarks (dark gray) and semilandmarks (light gray) digitized on the non-midsagittal region. For full anatomical descriptions of each numbered landmark see Table 3. Wireframes (black) used to display shape change are shown.

sis revealed highest slope values during infancy-childhood, decreasing thereafter to negligible values in adulthood (Fig. 3a, c). This analysis also showed a significant difference in the slopes between infancy-childhood and juvenility and non-significant differences between the rest of the consecutive age classes (Fig. 3a, c). However, for the base, there were significant differences in the slopes between adolescents and adults due to a decrease in size during adulthood (Fig. 3c). The Kruskal-Wallis test also yielded similar results for the vault and the base, with significant differences in size between infants-children and juveniles compared with adults (Table 6).

Table 4. Paired t test of Procruste coordinates of midsagittal landmarks.

Landmark number	x	y
1	0.34	–0.44
2	–0.59	–0.72
3	–0.55	–2.01
4	1.76	–1.95
5	1.39	1.61
6	0.91	0.89
7	–0.6	–1.56
8	–0.55	–2.65*
9	0.29	–1.74
10	2.05	2.02
11	–0.06	–1.15
12	1.36	–0.37
13	–0.96	1.35
14	–0.68	2.05
15	–0.59	–1.35
16	–0.88	0.55
17	0.3	–1.6
18	–0.38	–0.2
19	–1.28	0.79
20	–0.22	0.53
21	–0.89	1.76

Reference of landmark number in Fig. 1; *$p < 0.05$; **$p < 0.01$

Table 5. Paired t test of Procruste coordinates of non-midsagittal landmarks.

Landmark number	x	y	z
1	–0.68	1.39	–1.68
10	1.23	–1.4	2.56
19	–2.05	0.44	1.78
20	2.46	–0.57	–0.44
21	–0.66	3.44	2.44
22	1.76	0.66	0.32
23	0.76	0.44	–0.24
24	–2.34	–0.24	0.44
25	0.65	2.51	2.35
26	3.58*	3.01	4.00*
27	–1.67	2.58	–2.07
28	2.09	–1.34	2.16
29	–2.11	2.44	–0.55
30	2.06	1.45	2.11
31	0.66	–2.44	1.11
32	0.41	0.23	–2.57
33	2.45	0.48	2.51

Reference of landmark number in Fig. 2; *$p < 0.05$; **$p < 0.01$

The non-midsagittal features of the vault and base differed in growth trajectories. The vault only experienced major changes in size over the first 6 years of life (Fig. 3b). Regression analysis yielded sharp slopes for infancy-childhood and significant differences between this age class and juveniles (Fig. 3b). Although the cranial base exhibited a remarkable growth up to 6 years of age, it continued growing up to 12 years of age, with a higher slope value for infants-children and juveniles than for adolescents and adults (Fig. 3d). Just like for the vault, slope differences in size were only significant between infants-children and juveniles (Fig. 3d). The Kruskal-Wallis test indicated that vault size only differed significantly between infants-children and adults, while the base size showed significant differences between infants-children and juveniles compared with adults (Table 6).

Ontogenetic shape variation

For the midsagittal region, only PC1 – explaining 31.009% and 25.081% of the variation in vault and base shape, respectively – was significantly associated with age (r = 0.686 for the vault and r = 0.520 for the base). Overall, changes in shape indicate that the vault flattens and elongates in anteroposterior direction with increasing age (Fig. 4a). As a consequence, the frontal squama becomes more forwardly projected and the parietal is flattened and elongated, while the occipital squama is projected backwardly. Moreover, the vault bones increase in thickness (Fig. 4a). In the base, the cribriform plate is positioned into a more vertical orientation due to an upward displacement of the foramen cecum. The posterior height of the sphenoidal body shows an increase in the distance between Endo- and Ectosphenobasion. In addition, the Ectosphenobasion approaches the Hormion. The occipital clivus increases in length and thickness. On the nuchal plane, the Inion becomes thicker with age, separating from the Endinion (Fig. 4c). Figure 5 shows piecewise regression of scores for PC1. The vault developed gradually from infancy-childhood to adolescence (Fig. 5a) while the base developed gradually from infancy-childhood to the juvenile age class (Fig. 5c). Both the vault and base showed similar slopes from infancy-childhood to the juvenile age classes, with lower values for the base during adolescence (Fig. 5a, c). The regression analysis showed non-significant differences in the slopes between contiguous age classes (Fig. 5a, c), revealing a gradual change in shape.

In the non-midsagittal region, PC2 explained 29.462% of the variation in vault shape and was the only axis significantly associated with age (r = 0.671), while PC1 explained 21.247% of the variation in base shape and was the only

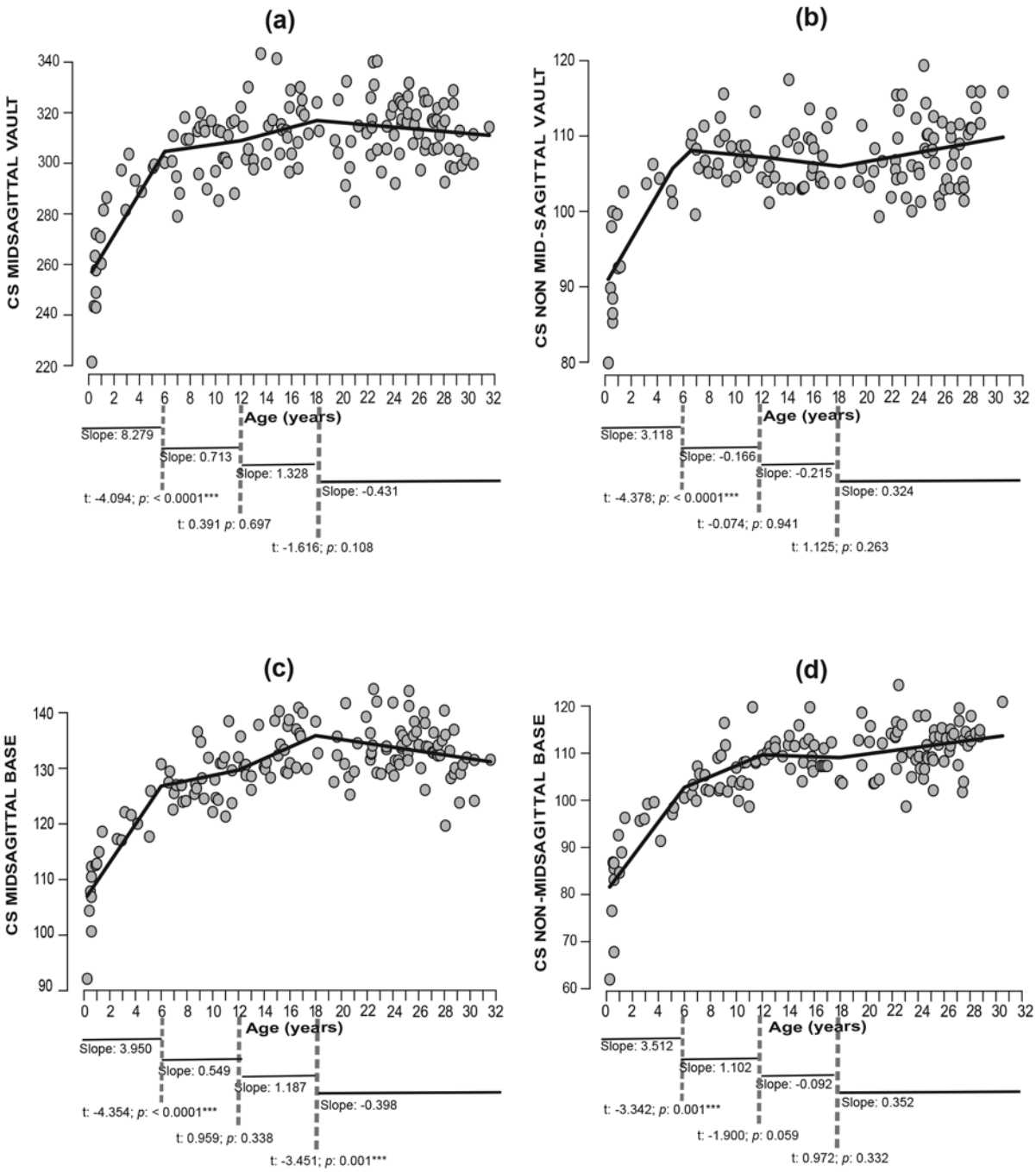

Fig. 3. Individual centroid size (CS) distribution. Lines were obtained by fitting data to a piecewise linear regression. Slope values for each age groups and statistical differences between groups are also shown.*$p < 0.05$; **$p < 0.01$.

axis significantly associated with age (r = 0.666). The most important ontogenetic changes in vault shape are as follows: the vault of younger individuals is more globular in shape than that of older ones. There is an outward displacement of the parietal wall and the larger cranial breadth is detected close to the base as age increases (Fig. 4b). The bones also become thicker, particularly in the lateral region close to the midline (Fig. 4b). In the base, PC1 showed that the middle fossa increases in length and breadth toward adulthood, with major changes taking place in the most lateral traits. As a consequence, the distance between the Sphenotemporal and the Posterior Zygomatic is increased due to a relative inward displacement of the Sphenotemporal and an outward displacement of the Posterior Zygomatic.

The piecewise regression analysis showed that the vault and the base followed very different trajectories of

Table 6. Results of the Kruskal-Wallis analysis of differences in Centroid Size between subadult groups and adults.

		Midsagittal		Non-midsagittal	
Age groups (years old)	**n**	**H**	***p***	**H**	***p***
			VAULT		
		H (all groups together): 49.082, $p < 0.001$		H (all groups together): 35.298, $p < 0.001$	
Infant-Child (0–5.99)	19	44.104	0.0001**	28.709	0.0001**
Juvenile 1 (6–7.99)	8	12.076	0.0001**	0.017	0.897
Juvenile 2 (8–9.99)	8	1.810	0.179	0.625	0.429
Juvenile 3 (10–11.99)	9	5.875	0.015*	0.092	0.762
Adolescent 1 (12–13.99)	9	0.085	0.770	3.395	0.065
Adolescent 2 (14–15.99)	11	0.025	0.875	0.006	0.938
Adolescent 3 (16–17.99)	7	0.057	0.811	0.007	0.933
			BASE		
		H (all groups together): 69.372, $p < 0.001$		H (all groups together): 69.780, $p < 0.001$	
Infant-Child (0–5.99)	19	52.859	0.000**	57.075	0.000**
Juvenile 1 (6–7.99)	8	10.683	0.001**	16.470	0.000**
Juvenile 2 (8–9.99)	8	5.677	0.017*	3.455	0.063
Juvenile 3 (10–11.99)	9	7.915	0.005**	7.669	0.006**
Adolescent 1 (12–13.99)	9	1.276	0.259	0.153	0.696
Adolescent 2 (14–15.99)	11	0.009	0.925	0.221	0.639
Adolescent 3 (16–17.99)	7	0.617	0.432	1.659	0.198

H: Kruskall-Wallis statistic; *$p < 0.05$; **$p < 0.01$

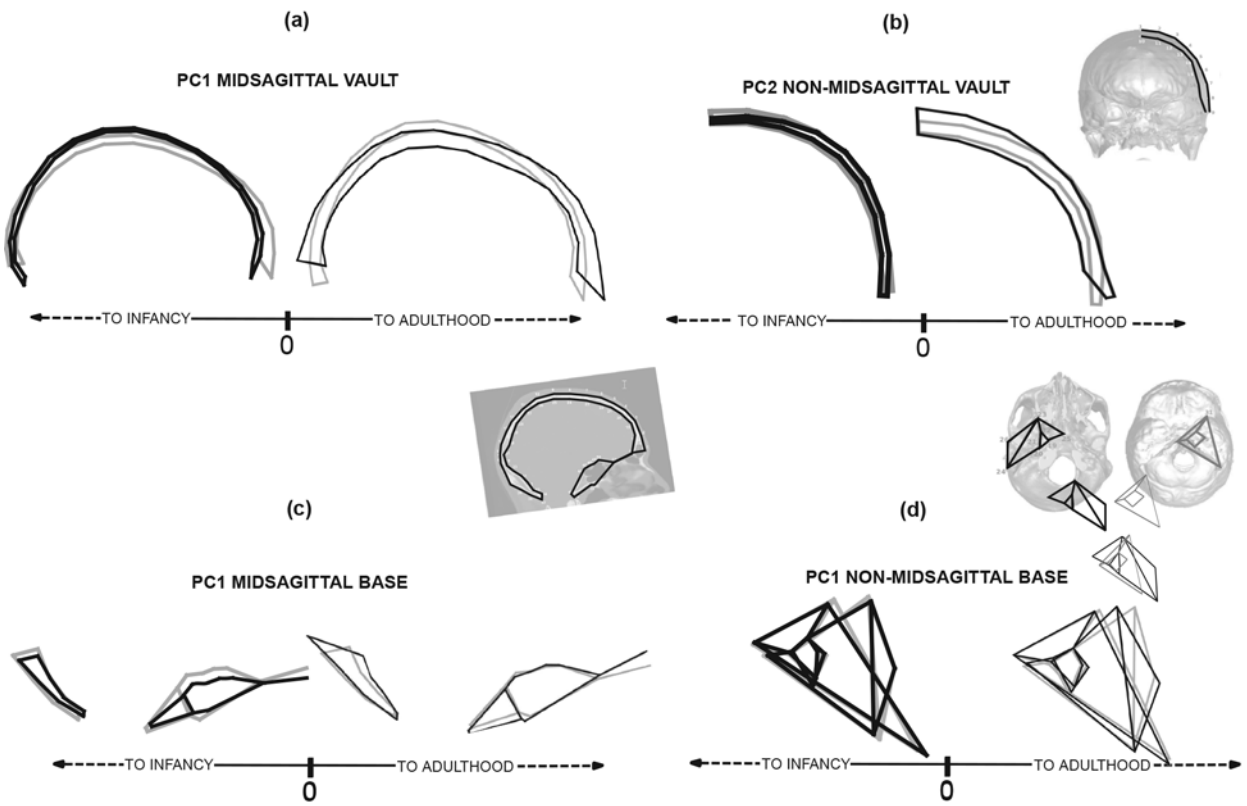

Fig. 4. Wireframe deformations along each principal component (PC) that was significantly correlated with age (r > 0.5). Gray line: mean reference shape. Black line: deformation of youngest (infants) and eldest (adults) individuals.

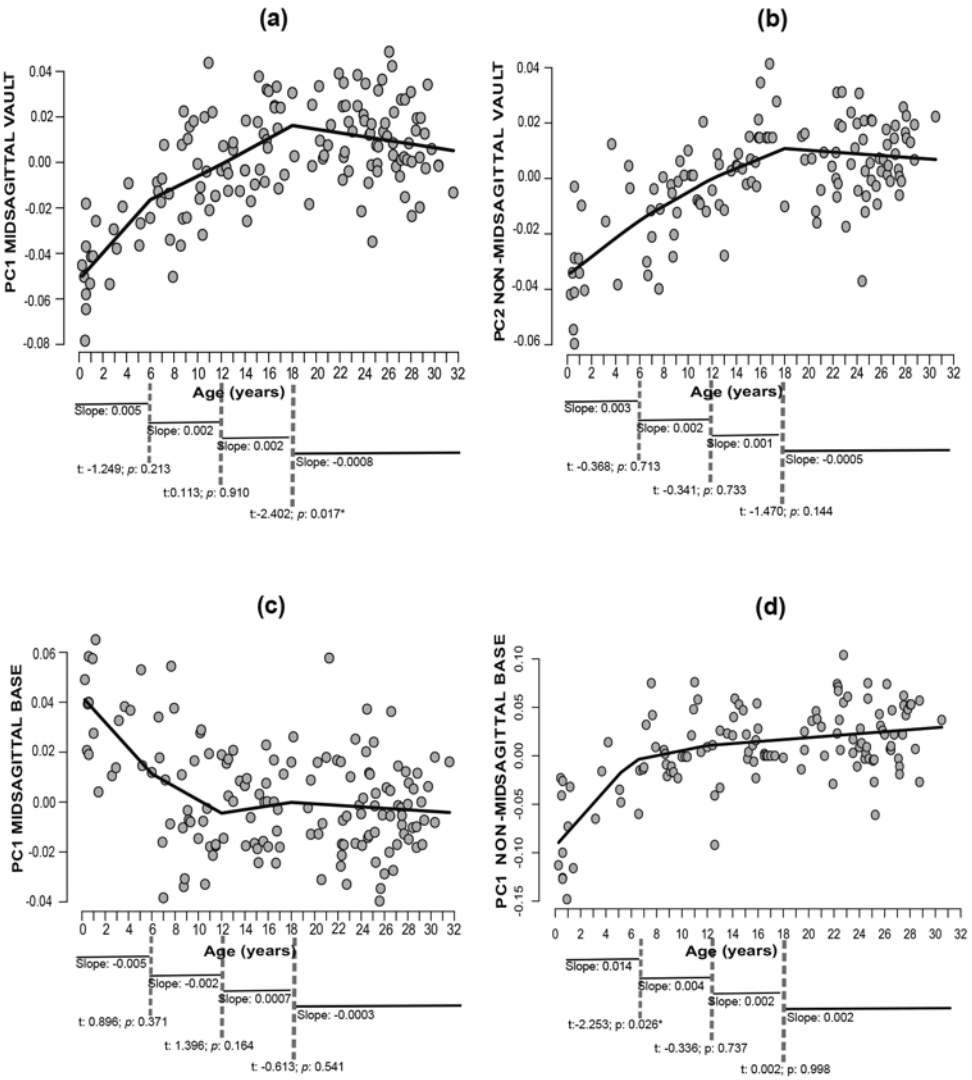

Fig. 5. Individual score distribution of principal components (PC). Lines were obtained by fitting data to a piecewise linear regression. Slope values for each age groups and statistical differences between groups are also shown.*$p < 0.05$; **$p < 0.01$.

shape. Vault shape changed gradually from infancy to early adulthood, with non-significant differences in the slopes between contiguous age classes (Fig. 5b). Conversely, the base underwent pronounced changes during the first 6 years of life (Fig. 5d), as indicated by the significant differences in the slope values between infancy-childhood and juvenility (Fig. 5d). The Kruskal-Wallis test showed consistent results, with significant differences in vault shape compared to adults until early adolescence (12–13.99 years old) and significant differences in the shape of the base between early juveniles (6–7.99 years old) and adults (Table 7).

Allometric shape changes

Figure 6a shows the ontogenetic trajectory of EV. It experienced a remarkable growth during the first 6 years of life and no changes thereafter (Fig. 6a). Accordingly, piecewise regression analysis showed significant changes in slopes only between the infancy-childhood and juvenility age classes (Fig. 6a). Linear regression analysis showed that changes in shape were significantly associated with changes in EV only for the infancy-childhood age class (Fig. 6b–e).

Sexual dimorphism

Figure 7 shows the trajectories of CS and the selected PCs for each sex. In the midsagittal region, the sizes of vault and base in males and females followed overlapping trajectories during infancy-childhood (Fig. 7a, c), differed significantly during juvenility and both regions were larger in adult males (Fig. 7a, c). In males the vault increased in size until late adolescence, while it stopped growing early in juvenile females (Fig. 7a). The base of males showed higher growth

Table 7. Results of the Kruskall-Wallis analysis of subadult groups compared with adults for the Principal Components correlated with age.

		Midsagittal		Non-midsagittal	
Age groups (years old)	**n**	**H**	***p***	**H**	***p***
			VAULT		
		H (all groups together): 60.473, $p < 0.001$		H (all groups together): 54.041, $p < 0.001$	
Infant-Child (0–5.99)	19	48.054	0.000**	29.368	0.000**
Juvenile 1 (6–7.99)	8	10.18	0.00**	21.738	0.000**
Juvenile 2 (8–9.99)	8	3.788	0.052	12.855	0.000**
Juvenile 3 (10–11.99)	9	3.246	0.072	4.458	0.035*
Adolescent 1 (12–13.99)	9	2.865	0.091	10.715	0.001**
Adolescent 2 (14–15.99)	11	0.802	0.370	0.01	0.922
Adolescent 3 (16–17.99)	7	0.685	0.408	3.108	0.065
			BASE		
		H (all groups together): 39.629, $p < 0.001$		H (all groups together): 46.192, $p < 0.001$	
Infant-Child (0–5.99)	19	30.422	0.000**	37.584	0.001**
Juvenile 1 (6–7.99)	8	1.143	0.285	4.360	0.037*
Juvenile 2 (8–9.99)	8	0.200	0.655	3.778	0.052
Juvenile 3 (10–11.99)	9	0.005	0.946	0.048	0.826
Adolescent 1 (12–13.99)	9	2.943	0.086	2.629	0.105
Adolescent 2 (14–15.99)	11	0.121	0.728	0.506	0.477
Adolescent 3 (16–17.99)	7	0.388	0.534	0.762	0.383

H: Kruskall-Wallis statistic; *$p < 0.05$; **$p < 0.01$

rates between the juvenility and adolescence age classes, resulting in significant differences between adult males and females (Fig. 7c). The regression analysis showed that midsagittal size was significantly different between sexes across ontogeny (t = 6.438, $p < 0.0001$ for the vault, t = 5.392, $p < 0.0001$ for the base). Non-midsagittal traits showed more overlapping of growth trajectories between sexes than did midsagittal traits (Fig. 7c, d). The regression analysis indicated non-significant variations in vault size (t = 1.210, $p = 0.229$) but significant ones in base size (t = 3.085, $p = 0.002$). The vault increased in size mainly during infancy-childhood, without significant changes thereafter (Fig. 7b). The base increased in size until juvenility (Fig. 7d) and continued to grow only in adult males (Fig. 7c, d).

In contrast to the results for size, no significant differences in shape were found between adult males and females (Fig. 7e–h). However, their developmental trajectories were not identical. In the midsagittal and non-midsagittal vault and base, females showed higher rates of development during infancy-childhood (Fig. 7e–h). Males showed more pronounced changes in vault shape during adolescence in the midsagittal region (Fig. 7e) and during juvenility in the non-midsagittal region (Fig. 7f). Some overlap was observed between sexes in the developmental trajectories of the base (Fig. 7g, h). The regression analysis, however, indicated non-significant differences between sexes for any of the PCs (t = −1.425, $p = 0.156$ and t = −0.221, $p = 0.825$ for PC1 of the midsagittal vault and base, respectively; t = 1.380, $p = 0.168$ and t = −0.082, $p = 0.934$ for the PC2 and PC1 of the non-midsagittal vault and base, respectively).

Discussion

In this work we found that the developmental trajectories of the neurocranium are non-linear, with varying growth rates throughout ontogeny. The most important changes occur during the first 6 years of postnatal life (Tables 6, 7; Figs 3, 5), although there are differences in size and shape between the vault and base. Our results support H1, which states that the midsagittal and non-midsagittal neurocranial regions show different ontogenetic trajectories but this was contrary to what we expected (see Introduction). Both vault regions showed different ontogenies but growth and development were similar between midsagittal and non-midsagittal structures of the base. In the vault, the midsagittal region attained

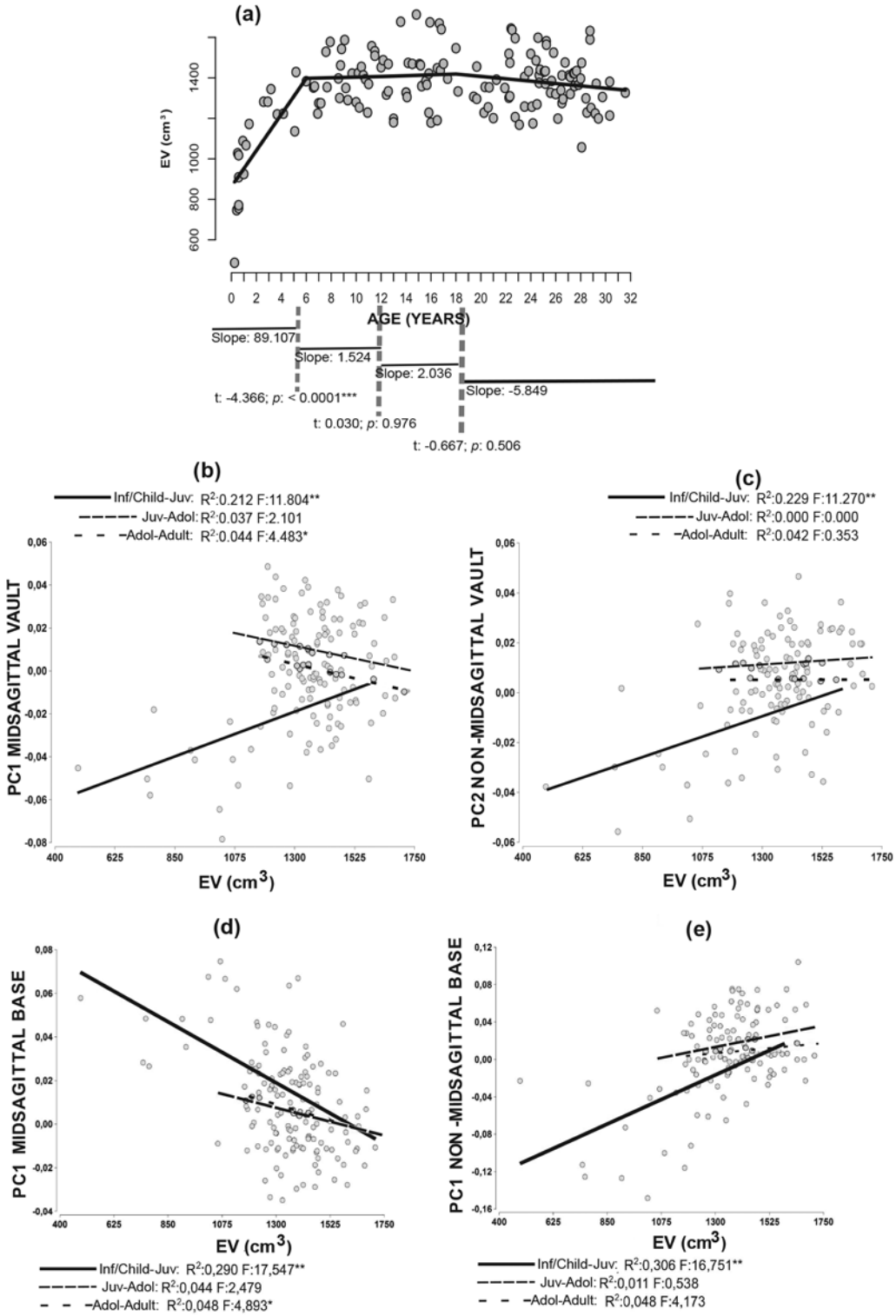

Fig. 6. **(a)** Individual EV distribution. Lines were obtained by fitting data to a piecewise linear regression. Slope values for each ontogenetic group and statistical differences between groups are also shown. *$p < 0.05$; **$p < 0.01$. **(b–e)** Individual score distribution of principal components (PC) versus EV. Lines were obtained by fitting data to a linear regression between contiguous age groups. Coefficient of determination (R^2) and F-statistics of regression are shown. *$p < 0.05$; **$p < 0.01$.

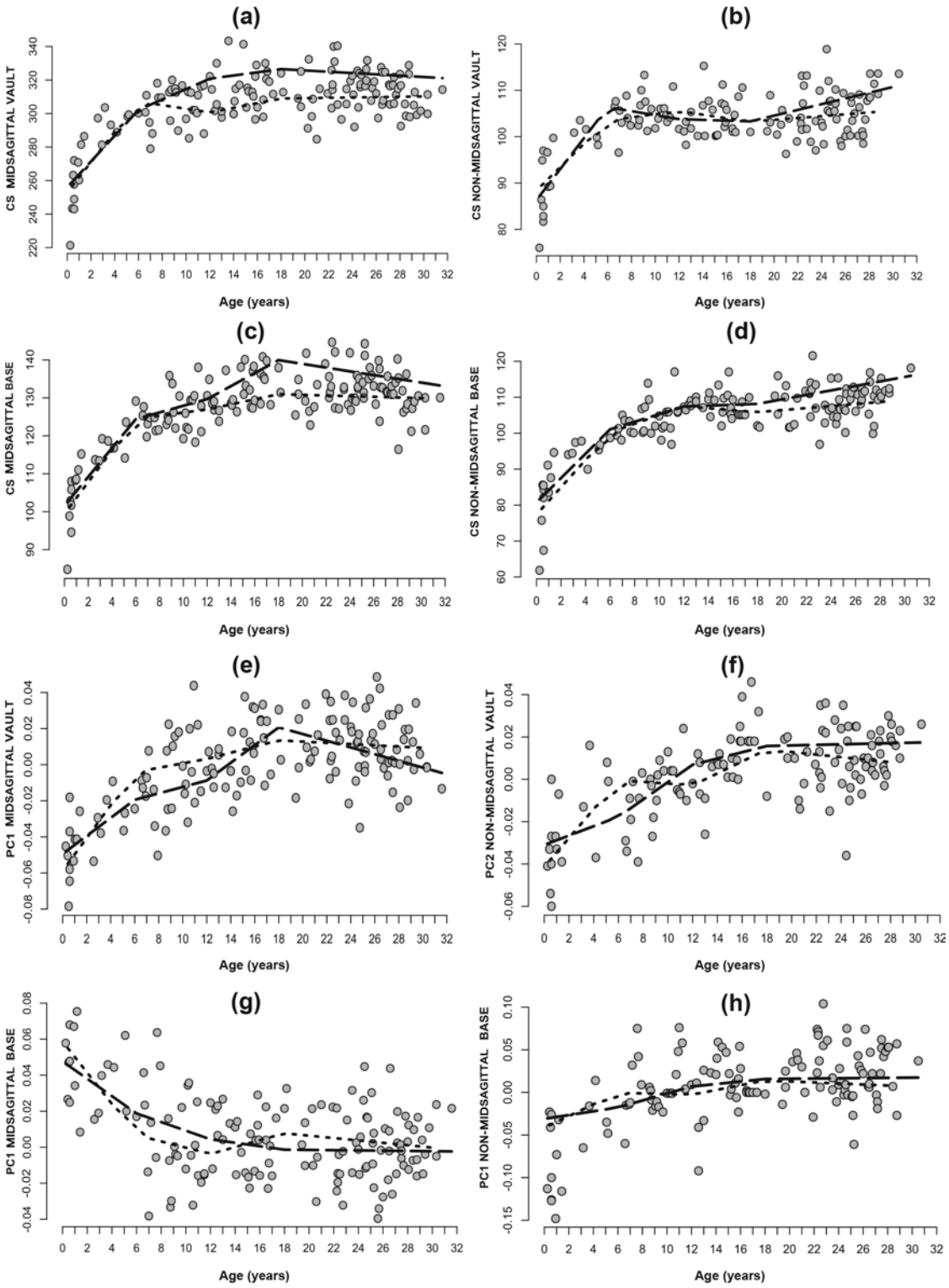

Fig. 7. Piecewise regression fitting for males and females. Dashed line: males. Dotted line: females.

adult size (10–11 years old, Table 6) after the non-midsagittal region, which attained adult size during infancy-childhood (Table 6, Fig. 3b). In contrast, for the shape, the non-midsagittal region showed changes until early adolescence (12–13 years old) (Table 7, Fig. 5b), while the midsagittal region reached adult shape earlier (6–7 years old, Table 7). In this case, according to expectations, non-midsagittal traits mature later than do midsagittal ones. Both in the midsagittal and non-midsagittal regions of the basicranium, the adult size is reached later (10–11 years old; Table 6, Fig. 3c, d) than does the adult shape (early juveniles; Table 7). These results are in disagreement with those obtained by Bastir et al. (2006), who analyzed sagittal and lateral ontogenies of the base and detected important differences between both regions, with lateral traits maturing later (during adolescence) than sagittal ones and in association with facial structures (e.g., mandible). However, such differences are probably due to the inclusion in the analysis of some landmarks and semilandmarks on the anterior cranial fossae.

We found that the main changes in size and shape of the analyzed neurocranial traits occur during infancy and childhood. Similar findings have been reported by Sardi & Ramirez-Rozzi (2005; 2007), who found that more than 90% of the size of different neurocranial regions is reached before 7 years of postnatal life. Neurocranial bones are influenced by their functional matrices, which are composed of soft tissues, organs and cavities (Moss & Young 1960). The brain is the most important neurocranial matrix and reaches about 80% of adult size by age 2 years and 95% by age 6 years (Lenroot & Giedd 2006; Giedd et al. 2009; Ventrice 2011). This may account for the significant association found in this study between all the morphometric variables and EV for infants and juveniles (Fig. 6), and may indicate, contrary to what we expected (see Introduction), that the brain influences not only midsagittal morphology, as already suggested (Bastir & Rosas 2005; Bastir et al. 2006), but also the non-midsagittal region. The loss of globularity from birth to adulthood (Fig. 4a) can be explained by the forward expansion of the frontal lobe and the flattening of the parietal lobes during brain growth (Trinkaus & LeMay 1982; Ventrice 2011). Another factor is osteogenesis at the sutures, the lambdoid suture being the site of more active growth (Trinkaus & LeMay 1982); this suture may affect changes at the level of the occipital squama (Fig. 4a). Brain expansion also stimulates bone growth at the sutures that run in anteroposterior direction, thus allowing an increase in vault breadth. The osteogenesis at the sutures causes the bones to be less curved (Enlow 1990), which contributes to the loss of globularity (Fig. 4).

In the basicranium, the three synchondroses exhibit some anteroposterior elongation (Opperman et al. 2005). However, the most important midsagittal changes in adults are the downward position of the base and an increase in the length of the occipital clivus (Fig. 4c). In this case, brain growth activates processes of resorption of the inner surface and deposition on the outer surface (Enlow 1990). Bone deposition at the anterior margin of the foramen magnum causes it to be more obliquely inclined (Fig. 4c). These processes contrast with those in the vault, which becomes thicker by osteogenesis on both surfaces.

The ontogenetic variation in non-midsagittal structures can be explained by the fact that the middle fossae of the basicranial region contain the temporal lobes (Bastir & Rosas 2008). It has been suggested that the temporal lobe volume scales isometrically with the fossa indicating developmental integration (Richtsmeier et al. 2006; Sperber 2010). The growth of the temporal lobe stimulates sutural osteogenesis, promoting a remarkable increase in fossa breadth (Fig. 4d), bone resorption of the anterior surface of the fossa and deposition at the Sphenofrontal suture, providing space for facial development.

In this way, brain growth emerges as a factor that integrates the morphology of both regions early in ontogeny, showing coordinated changes due to ontogenetic allometry (Lieberman et al. 2000; Hallgrímsson et al. 2007; Porto et al. 2009; Barbeito-Andrés et al. 2015). Endocranial volume (i.e. brain) stops growing during childhood (Ventrice 2011) (Fig. 6a). However, after childhood some significant changes continue to take place in the midsagittal vault size, base size and non-midsagittal vault shape (Tables 6, 7; Fig. 3a, c, 4b). This emphasizes the need to identify other factors affecting the morphology of midsagittal and non-midsagittal traits.

We observed a greater-than-expected extension of the growth trajectory of the midsagittal vault, probably resulting from the influence of bone thickness (Table 6, Figs. 3a, b). Anzelmo et al. (2014) stated that the midsagittal region is much thicker than the lateral walls because of its higher growth rate during the first years of life. Both midsagittal and non-midsagittal regions of the base attain adult size by the late juvenile period (Table 6; Fig. 3c, d), but this may be accomplished by different factors. Midsagittal growth occurs at the Sphenooccipital synchondrosis, which presents osteogenic activity until puberty even after the brain has reached its full size. This synchondrosis is responsible for basicranial elongation until it fuses between 12–15 years of age (Enlow 1990; Sperber 2010). It is well known that different parts of the brain differ in growth rate and time of change (Enlow 1990; Giedd et al. 2009). In this regard, the temporal lobes attain adult size much later than do the parietal and frontal lobes (Enlow & Hans 1996; Gogtay et al. 2004). Such behavior of the temporal lobes may explain why the development of the non-midsagittal vault region continues until adolescence (Table 7; Fig. 5b). The lateral walls articulate with the lateral base, which expands until late ontogenetic stages; this may affect vault breadth which, in adults, is located in a more downward position near the suture with the temporal bone (Fig. 4b).

It has been a matter of debate whether mastication influences the generation of a modular neurocranial pattern (Bastir et al. 2005; Bastir et al. 2006). Our results do not support

the idea that the organizational patterns of the midsagittal and non-midsagittal regions are completely independent from each other. Although chewing-related structures such as bones and muscles would also affect the morphology of the lateral neurocranium by, for example, stimulating bone thickness in the midsagittal region, it may not be enough to generate different patterns of modular organization.

In relation to sexual dimorphism, we observed similar ontogenetic trajectories between sexes (Fig. 7), except for the size in the midsagittal region, where males showed larger structures than females during late ontogeny possibly due to a longer growth period which continues after infancy-childhood (Fig. 7a, c). In contrast, Bulygina et al. (2006) detected early sexual dimorphism in the midsagittal plane of the frontal bone and assumed the occurrence of prenatal differences in the size of the neurocranium between sexes. Differences between studies can be explained by the fact that we included in the analysis other parts of the midsagittal plane and the variation in the size of the basicranium. In the non-midsagittal region, the ontogenetic trajectory of the vault (Fig.7b) and base (Fig.7d) showed overlapping between males and females. Although these trajectories seemed to diverge between adolescence and adulthood, the Kruskal-Wallis test indicated that the vault attains adult size in infancy-childhood, and the base in the late juvenile age class (Table 6). It is possible that the late changes seen in the growth trajectory of males are a methodological artifact.

A large proportion of sexual dimorphism in the shape of the skull has been attributed to ontogenetic scaling, with males growing further along a trajectory shared by the juveniles and adults of both sexes (Leigh & Cheverud 1991). Ontogenetic scaling would account for sexual dimorphism in the face (Rosas & Bastir 2002; Bulygina et al. 2006; Anzelmo et al. 2012), but not in the neurocranium, where size variations between sexes were not associated with shape variations. According to our results, H2, which states that the neurocranium of males and females follow different ontogenetic trajectories can be rejected for sexual dimorphism in shape but not in size.

Conclusions

In this study we made an ontogenetic analysis of several factors that are potentially involved in the morphological variation of the cranial vault and base from a developmental framework. Our results reveal minor differences in the ontogenetic trajectories between the midsagittal and non-midsagittal regions. In both of them, considerable shape and size changes may occur early in postnatal life, with adult values being reached by the end of the juvenile stage, except for the further development of the lateral vault region. Thus, the results presented here and those of previous studies (Bastir et al. 2005; Bastir et al. 2008) can be better explained by variations between the different brain regions. In contrast, the effect of bony structures and muscles related to chewing might not have been strong enough to induce significant and independent modifications in lateral structures. Furthermore, the influence of masticatory muscles attached to the external surface on neurocranial morphology appears to have been smaller than that exerted by muscles on the postcranial skeleton (Rawlinson et al. 1995).

The large human brain and the scarce influence of the muscles on the neurocranium could have generated a quite integrated structure in humans. This study contributed to a better understanding of the role the brain might have played in the evolutionary changes of the midsagittal and non-midsagittal regions.

Acknowledgements: We thank the Fundación para la Lucha contra las Enfermedades Neurológicas de la Infancia (FLENI) for providing the tools to build the database used in this work. We also thank Federico Lotto and Silvia Pietrokovsky for improving the use of English.

References

Ackermann, R.R. & Krovitz, G.E. (2002): Common patterns of facial ontogeny in the hominid lineage. – Anat. Rec. 269: 142–147.

Anzelmo, M., Sardi, M.L., Barbeito-Andrés, J. & Pucciarelli, H.M. (2012): Alometrías ontogénicas y dimorfismo sexual facial en dos poblaciones humanas modernas. – Rev. Arg. Antrop. Biol. 14 (1): 89–100.

Anzelmo, M., Barbeito-Andrés, J., Ventrice, F., Pucciarelli, H.M. & Sardi, M.L. (2013): Ontogenetic patterns of morphological variation in the ectocranial human vault. – Anat. Rec. 296: 1008–1015.

Anzelmo, M., Ventrice, F., Barbeito-Andres, J., Pucciarelli, H.M. & Sardi, M.L. (2014): Ontogenetic changes in cranial vault thickness in a modern sample of *Homo Sapiens*. – Am. J. Hum. Biol. 27: 475–485.

Arnqvist, G. & Martensson, T. (1998): Measurement error in geometric morphometrics: empirical strategies to assess and reduce. – Acta Zool. Acad. Sci. Hung. 44: 73–96.

Balzeau, A. (2006): Are thickened cranial bones and equal participation of the three structural bone layers autapomorphic traits of *Homo erectus*? – Bull. Mem. Soc. Anthrop. Paris 18: 145–163.

Barbeito-Andrés, J., Ventrice, F., Anzelmo, M., Pucciarelli, H.M. & Sardi, M.L. (2015): Developmental covariation of human vault and base throughout postnatal ontogeny. – Ann. Anat. 197: 59–66.

Bastir, M. & Rosas, A. (2005): Hierarchical nature of morphological integration and modularity in the human posterior face. – Am. J. Phys. Anthropol. 128 (1): 26–34.

Bastir, M. & Rosas, A. (2006): Correlated variation between the lateral basicranium and the face: a geometric morphometric study in different human groups. – Arch. Oral. Biol. 51 (9): 814–824.

Bastir, M. & Rosas, A. (2008): Mosaic evolution, integration and modularity: evolution of the human cranial base. – Am. J. Phys. Anthropol. S46: 65.

Bastir, M. & Rosas, A. (2009): Mosaic evolution of the basicranium in Homo and its relation to modular development. – Evol. Biol. 36 (1): 57–70.

Bastir, M., O'Higgins, P. & Rosas, A. (2005): Human evolution: relationships between the basicranium and the face. – Ann. Hum. Biol. 32: 790.

Bastir, M., Rosas, A. & O'Higgins, P. (2006): Craniofacial levels and the morphological maturation of the human skull. – J. Anat. 209: 637–654.

Bastir, M., Rosas, A., Lieberman, D.E. & O'Higgins, P. (2008): Middle cranial fossa anatomy and the origins of modern humans. – Anat. Rec. 291 (2): 130–140.

Baughan, B. & Demirjian, A. (1978): Sexual dimorphism in the growth of the cranium. – Am. J. Phys. Anthropol. 49 (3): 383–390.

Baughan, B., Demirjian, A., Levesque, G.Y. & Lapalme-Chaput, L. (1979): The pattern of facial growth before and during puberty, as shown by French-Canadian girls. – Ann. Hum. Biol. 6: 59–76.

Bienvenu, T., Guy, F., Coudyzer, W., Gilissen, E., Roualdès, G., Vignaud, P. & Brunet, M. (2011): Assessing endocranial variations in great apes and humans using 3D data from virtual endocasts. – Am. J. Phys. Anthropol. 145: 231–246.

Bogin, B. (1999): Patterns of human growth. – Cambridge University Press, Cambridge.

Bogin, B. (2003): The human pattern of growth and development in paleontological perspective. – In: Thompson, J.L., Krovitz, G.E. & Nelson, A.J. (eds): Patterns of growth and development in the genus *Homo*. – Cambridge University Press, Cambridge, pp. 15–44.

Bookstein, F., Schafer, K., Prossinger, H., Seidler, H., Fieder, M., Stringer, C., Weber, G.W., Arsuaga, J.L., Slice, D.E., Rohlf, F.J., Recheis, W., Mariam, A.J. & Marcus, L.F. (1999): Comparing frontal cranial profiles in archaic and modern *Homo* by morphometric analysis. – Anat. Rec. 257: 217–224.

Bookstein, F., Gunz, P., Mitteroecker, P., Prossinger, H., Schaefer, K. & Seidler, H. (2003): Cranial integration in *Homo*: singular warps analysis of the midmidsagittal plane in ontogeny and evolution. – J. Hum. Evol. 44: 167–187.

Bruner, E., Saracino, B., Passarello, P., Ricci, F., Tafuri, M. & Manzi, G. (2004): Midmidsagittal cranial shape variation in the genus Homo by geometric morphometrics. – Coll. Antropol. 28: 99–112.

Buikstra, J. & Ubelaker, D. (1994): Standards for data collection from human skeletal remains. – Arkansas Archaeological Survey Research Series 44, Fayetteville.

Bulygina, E., Mitteroecker, P. & Aiello, L. (2006): Ontogeny of facial dimorphism and patterns of individual development within one human population. – Am. J. Phys. Anthropol. 131 (3): 432–443.

Buschang, P.H. & Hinton, R.J. (2005): A gradient of potential formodifying craniofacial growth. – Sem. Orthod. 11: 219–226.

Conroy, G.C., Weber, G.W., Seidler, H., Recheis, W., zur Nedden, D. & Mariam, J.H. (2000): Endocranial capacity of the Bodo cranium determined from three-dimensional computed tomography. – Am. J. Phys. Anthropol. 113: 111–118.

Enlow, D.H. (1990): Facial growth. – WB Saunders, Philadelphia.

Enlow, D.H. & Hans, M.G. (1996): Essentials of facial growth. – WB Saunders, Philadelphia.

Giedd, J.N., Lalonde, F.M., Celano, M.J., White, S.L., Wallace, G.L., Lee, N.R. & Lenroot, R.K. (2009): Anatomical brain magnetic resonance imaging of typically developing children and adolescents. – J. Am. Acad. Child. Adolesc. Psychiat. 48 (5): 465–470.

Gogtay, N., Giedd, J.N., Lusk, L., Hayashi, K.M., Greenstein, D., Vaituzis, A.C., Nugent III, T.F., Herman, D.H., Clasen, L.S., Toga, A.W., Rapoport, J.L. & Thompson, P.M. (2004): Dynamic mapping of human cortical development during childhood through early adulthood. – Proc. Natl. Acad. Sci. USA 101 (21): 8174–8179.

González, P.N., Bernal, V. & Perez, S.I. (2009): Analysis of sexual dimorphism of craniofacial traits using geometric morphometric techniques. – Int. J. Osteoarchaeol. 21: 82–91.

Guihard-Costa, A. & Ramirez-Rozzi, F. (2004): Growth of the human brain and skull slows down at about 2.5 years old. – C. R. Palevol. 3: 397–402.

Gunz, P., Mitteroecker, P. & Bookstein F.L. (2005): Semilandmarks in three dimensions. – In: Slice, D.E. (ed): Modern Morphometrics in Physical Anthropology. – Kluwer Academic/ Plenum Publishers, New York, pp. 73–98.

Hallgrímsson, B., Lieberman, D.E., Liu, W., Hutchinson, A.F. & Jirik, F.R. (2007): Epigenetic interactions and the structure of phenotypic variation in the cranium. – Evol. Dev. 9: 76–91.

Howells, W.W. (1973): Cranial Variation in Man. A Study by Multivariate Analysis of Patterns of Differences Among Recent Human Populations. – Papers Peabody Mus. 67: 259.

Humphrey, L.T. (1998): Growth patterns in the modern human skeleton. – Am. J. Phys. Anthropol. 105: 57–72.

Imbelloni, J. (1938): Tabla clasificatoria de los indios regiones biológicas y grupos raciales humanos de América. – Physis. 12: 229–249.

Kendall, D.G. (1977): The diffusion of shape. – Adv. Appl. Prob. 9: 428–430.

Klingenberg, C.P. (2003): Quantitative genetics of geometric shape: heritability and the pitfalls of the univariate approach. – Evol. 57: 191–195.

Klingenberg, C.P. (2009): Morphometric integration and modularity in configurations of landmarks: tools for evaluating a priori hypotheses. – Evol. Dev. 11 (4): 405–421.

Klingenberg, C.P. (2016): Size, shape, and form: concepts of allometry in geometric morphometrics. – Dev. Genes Evol. 226: 113–137.

Leigh, S.R. & Cheverud, J.M. (1991): Sexual dimorphism in the baboon facial skeleton. – Am. J. Phys. Anthropol. 84 (2): 193–208.

Lenroot, R.K. & Giedd, J.N. (2006): Brain development in children and adolescents: insights from anatomical magnetic resonance imaging. – Neurosci. Biobehav. Rev. 30 (6): 718–729.

Lieberman, D.E., Ross, C.F. & Ravosa, M.J. (2000): The primate cranial base: ontogeny, function, and integration. – Yb. Phys. Anthropol. 43: 117–169.

Lieberman, D.E., McBratney, B.M. & Krovitz, G.E. (2002): The evolution and development of cranial form in *Homo sapiens*. – PNAS 99 (3): 1134–1139.

Lieberman, D.E., Krovitz, G.E., Yates, F.W., Devlin, M. & St Claire, M. (2004): Effects of food processing on masticatory strain and craniofacial growth in a retrognathic face. – J. Hum. Evol. 46 (6): 655–677.

Mitteroecker, P., Gunz, P. & Bookstein, F.L. (2005): Heterochrony and geometric morphometrics: a comparison of cranial growth

in Pan paniscus versus Pan troglodytes. – Evol. Dev. 7: 244–258.

Moss, M.L. & Young, R.W. (1960): A functional approach to craniology. – Am. J. Phys. Anthropol. 18 (4): 281–292.

Neubauer, S., Gunz, P. & Hublin, J.-J. (2009): The pattern of endocranial ontogenetic shape changes in humans. – J. Anat. 215 (3): 240–255.

Neubauer, S., Gunz, P. & Hublin, J.-J. (2010): Endocranial shape changes during growth in chimpanzees and humans: a morphometric analysis of unique and shared aspects. – J. Hum. Evol. 59 (5): 555–566.

Opperman, L.A., Gakunga, P.T. & Carlson, D.S. (2005): Genetic factors influencing morphogenesis and growth of sutures and synchondroses in the craniofacial complex. – Semin. Orthod. 11: 199–208.

Porto, A., Oliveira, F.B., Shirai, L.T., Conto, V. & Marroig, G. (2009): The evolution of modularity in the mammalian skull I: morphological integration patterns and magnitudes. – Evol. Biol. 36: 118–135.

Rawlinson, S.C.F., Mosley, J.R., Suswillo, R.F.L., Pitsillides, A.A. & Lanyon, L.E. (1995): Calvarial and limb bone cells in organ and monolayer culture do not show the same early responses to dynamic mechanical strain. – J. Bone Min. Res. 10: 1225–1232.

Reddy, D.P., Harvati, K. & Kim, J. (2004): An alternative approach to space curve analysis using the example of the Neanderthal occipital bun. – In: Slice, D.E. (ed.): Modern morphometrics in Physical Anthropology. – Kluwer Academic/Plenum Publishers, New York, pp. 99–115.

Richtsmeier, J.T., Corner, B.D., Grausz, H.M., Cheverud, J.M. & Danahey, S.E. (1993): The role of postnatal growth pattern in the production of facial morphology. – Syst. Biol. 42: 307–330.

Richtsmeier, J.T., Aldridge, K., DeLeon, V.B., Panchal, J., Kane, A.A., Marsh, J.L., Yan, P. & Cole, T.M. (2006): Phenotypic integration of neurocranium and brain. – J. Exp. Zool. B. Mol. Dev. Evol. 306: 360–378.

Ricklan, D.E. & Tobias, P.V. (1986): Unusually low sexual dimorphism of endocranial capacity in a Zulu cranial series. – Am. J. Phys. Anthropol. 71: 285–293.

Rosas, A. & Bastir, M. (2002): Thin-plate spline analysis of allometry and sexual dimorphism in the human craniofacial complex. – Am. J. Phys. Anthropol. 117 (3): 236–245.

Rushton, J.P. (1992): Cranial capacity related to sex, rank, and race in a stratified random sample of 6,325 U.S. military personnel. – Intelligence 16: 401–413.

Sardi, M.L. & Ramírez-Rozzi, F. (2005): A cross-sectional study of human craniofacial growth. – Ann. Hum. Biol. 32: 390–396.

Sardi, M.L. & Ramírez-Rozzi, F. (2007): Developmental connections between cranial components and the emergence of the first permanent molar in humans. – J. Anat. 210: 406–417.

Sardi, M.L., Barbeito-Andrés, J., Ventrice, F., Ramírez-Rozzi, F., Anzelmo, M. & Guihard-Costa, A.-M. (2014): Covariación ontogénica en el endocráneo de Pan troglodytes. – Rev. Arg. Antrop. Biol. 16 (2): 79–91.

Sperber, G.H. (2010): Craniofacial development and growth. – People Medical Publishing House, Shelton.

Spoor, F., Jeffery, N. & Zonneveld, F. (2000): Imaging skeletal growth and evolution. – In: O'Higgins, P. (ed.): Development, growth and evolution. – The Linnaean Society of London, London, pp. 123–161.

Strand-Vidarsdóttir, U. & O'Higgins, P. (2001): Development of sexual dimorphism in the facial skeleton of anatomically modern Homo sapiens. – Am. J. Phys. Anthropol. 114: 139–152.

Strand-Vidarsdottir, U., O'Higgins, P. & Stringer, C.B. (2002): A geometric morphometric study of regional differences in the growth of the modern human facial skeleton. – J. Anat. 201: 211–229.

Trinkaus, E. & LeMay, M. (1982): Occipital bunning among later Pleistocene hominids. – Am. J. Phys. Anthropol. 57: 27–35.

Ventrice, F. (2011): Modern human brain growth and development. Contribution to brain evolution in hominins. – PhD Thesis. Universität Zürich, Zurich.

Vieth, E. (1989): Fitting piecewise linear regression functions to biological responses. – J. App. Phys. 67: 390–396.

Zelditch, M., Swiderski, D.L., Shetts, H.D. & Finks, W.L. (2004): Geometric Morphometrics for Biologists: A Primer. – Elsevier Academic Press, Amsterdam.

Zollikofer, C.P.E., Bienvenu, T. & Ponce de León, M.S. (2016): Effects of cranial integration on hominid endocranial shape. – J. Anat. 230: 85–105.

Manuscript received: 27 April 2017
Revisions required: 21 September 2017
Revised version received: 20 December 2017
Accepted: 03 January 2018